#### A SIMPLE MODEL FOR TWO-PHASE SLUG FLOW INDUCED DAMPING

N.W. Mureithi<sup>1</sup>, T.P. Sawadogo<sup>1</sup> and F. Bernard<sup>2</sup>

<sup>1</sup> BWC/AECL.NSERC Chair of Fluid-Structure Interaction
Ecole Polytechnique, Montreal, Canada

<sup>2</sup> ENSEEIHT, Toulouse, France
njuki.mureithi@polymtl.ca, fabien.bernard@alumni.enseeiht.fr,
teguewinde-pierre.sawadogo@polymtl.ca

#### **Abstract**

The two-phase flows are prevalent in various industrial fields such as nuclear engineering, chemical engineering and the petroleum industry. At high speeds, flows through piping may generate significant excitation forces, particularly at joints and bends in piping systems. Interestingly, the flows may also generate significant damping forces which can be desirable from a vibration damping point of view.

The question of exactly how internal two-phase flows generate damping remains largely unanswered. Indeed so is the question for external two-phase flows, which are even more complex. The problem addressed in this study is related to the behavior of tubular structures subjected to internal two-phase slug flow or nearly slug flow. The observation of slug flow subjected to transverse vibration led to consideration of the effects of sloshing liquid slugs due to the external vibration. Indeed, in flow visualization tests, the upper free surface of the slugs in vertical flow was found to deform significantly as the tube vibrated. This suggested a possible mechanism for energy transfer from the structure to the fluid which could be (at least partially) responsible for the observed two-phase flow-induced damping.

An analytical model is developed aimed at incorporating the most basic sloshing effects of liquid slugs travelling through a tube at low speed. The first part of the work demonstrates that considering slugs as as simple points masses travelling through the tube leads only to low energy transfer from the tube to the flow and thus cannot explain the level of energy transfer observed in experimental damping tests.

In the second part of the work, the flow dynamics within the slug are modeled to account for linear order free surface oscillations related to first mode sloshing. Numerical solution of the resulting equations shows that the energy transfer is much higher and results in damping levels of the same order as found in experimental measurements. The results suggest that sloshing of the individual slugs is an important mechanism of energy transfer for slug flow.

The analytical results are in qualitative agreement with experimental measurements. In view of the simplicity of the model, the results are encouraging. The model can, however, be improved to better represent more details of the flow.

#### Introduction

Two-phase flow-induced damping is one of the important phenomena resulting from the interaction between structures (here pipes or tubes) and two-phase flows. This type of damping is of practical significance since it positively works to reduce vibrations of piping carrying the two-phase flow

mixtures. Yet, besides this inherent advantage, particularly for high speed flows, the mechanisms underlying two-phase flow damping remain largely unknown. Significant work has been done identifying key properties of two-phase damping, e.g. [1]-[5]. The work of [2], dealing primarily with external cross-flow, shows that two-phase damping attains a maximum value near a superficial void fraction (or volumetric quality) of 50-60%. Interestingly, a very similar trend is found for internal two-phase flows as we see later.

Fig.1 shows some typical flow patterns in vertical internal two-phase flows. Pattern (a) corresponds to bubbly flow. For the bubbly flow regime (in the range 5-20% void fraction) the authors of [3] found that the two-phase damping correlated very well to the total interface surface area of the gas bubbles in the mixture.

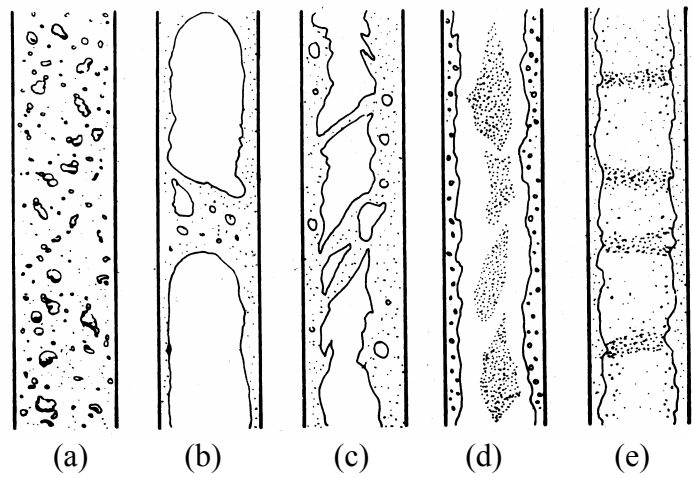


Figure 1 Flow regimes in upward two-phase flow in vertical tubes: (a) Bubbly flow, (b) Slug flow, (c) Churn flow, (d) Wispy-annular flow, (e) Annular flow (Collier and Thome, [5])

In the present work particular interest is paid to pattern (b) referred to as slug flow. In slug flow, elongated air bubbles are interspersed with fairly well defined liquid slugs. This nearly discrete flow structure renders itself amenable to the simplified analysis considered here. Despite the existence of experimental correlations for two-phase damping, fundamental research on the underlying mechanisms of two phase damping remains limited. The present work aims to take advantage of the simpler structure of slugs to develop simple theoretical models that could shed light on the fundamental nature of two-phase damping of tubes or pipes carrying slug flow.

# 1. Slug flow model and fluid-structure system

## 1.1 Slug flow model

The goal of the present study is to investigate how discrete discontinuities in the fluid density, in the form of slugs, lead to transfer of energy from the structure to the flow resulting in an effective damping of the containing tube vibrations. For this purpose, the approach taken is to model the fluid mechanics in the simplest fashion possible. The flow itself is modelled as a plug flow as is often

done for internal pipe flows when studying internal flow induced vibrations [6]. In the present case, however, the existence of two phases must be taken into account.

For given flow conditions, a slug distribution as depicted in Fig.2 is considered. Vertical upward flow will be considered; the tube is shown horizontal here for convenience. Slug size and number of slugs (slug frequency) are estimated from experimental data. In order to write the equation of motion of the pipe subjected to axial slug flow, an analytical expression for the mass distribution in the pipe as a function of time is needed. Referring to Fig.2, slugs are formed at a frequency f = 1/T. Gas bubbles are considered to be of negligible mass and incompressible. Liquid slugs are identical and have mass  $m_0$ . A slug entering the tube at time t=0 will be located at the position x=Ut at time t; here t is the average slug speed. Using the Dirac delta function, the mass distribution function associated with the slug may be expressed as t0 and t1. At a given instant, the total number of slugs in the tube of length t1 is t2.

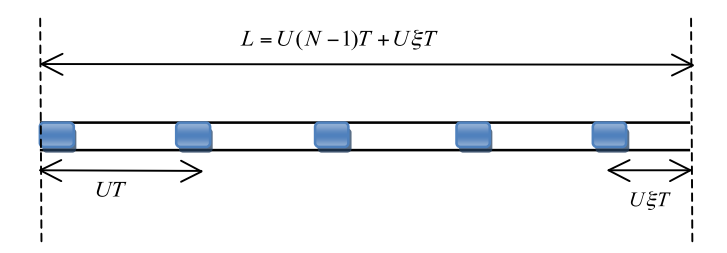


Figure 2 Instantaneous slug distribution in a pipe of length L.

The total mass distribution associated with the *N* slugs is therefore

$$m(x,t) = m_0 \sum_{i=1}^{N-1} \delta(U(i-1)T + x - Ut) + m_0 \delta(U(N-1)T + x - Ut)h(1 - \frac{t}{\xi T})$$
(1)

where the factor  $\xi$  represents a partial length as shown in Fig.1 and h(.) is the Heaviside function.

# 1.2 Fluid-structure system equations

We consider next the equation of motion of the fluid-structure system. The system under consideration is a pinned-pinned (or later, clamped-clamped) tube subjected to internal two phase flow. Fig.3 shows a section of the tube with internal flow under consideration.

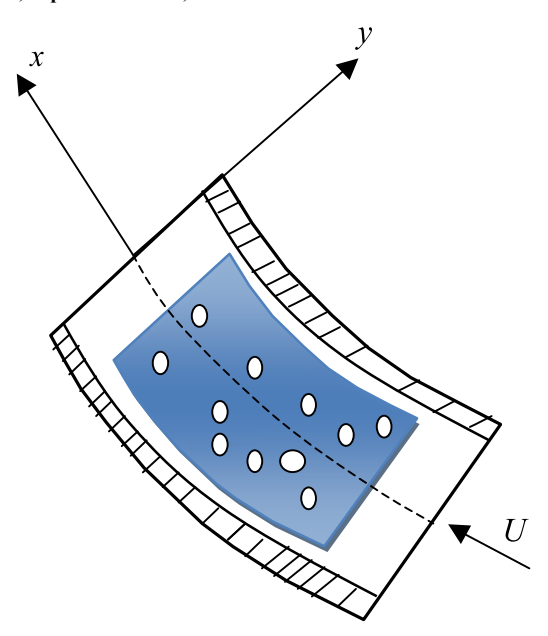


Figure 3 Fluid-structure element.

The tube has mass per unit length M, structural rigidity EI and total length L. The resulting equation of motion [6] is

$$EI\frac{\partial^{4}y}{\partial x^{4}} + (M+m)\frac{\partial^{2}y}{\partial t^{2}} + 2mU^{2}\frac{\partial}{\partial t}\left(\frac{\partial y}{\partial x}\right) + \left(U^{2}m(L,t) + I(x,t)\right)\frac{\partial^{2}y}{\partial x^{2}} + \left(\frac{\partial m}{\partial t} + U\frac{\partial m}{\partial x}\right)\left(\frac{\partial y}{\partial t} + U\frac{\partial^{2}y}{\partial x^{2}}\right) = 0 \quad (2)$$

where the fluid mass m(x,t) is given by equation (1) and  $I(x,t) = \int_{x}^{L} \left( U \frac{\partial m}{\partial t} + m \frac{\partial U}{\partial t} \right) dx$ .

## 1.3 Simplified analysis

Introducing the modal expansion

$$y(x,t) = \sum_{i} \varphi_{i}(x)q_{i}(t)$$
(3)

equation (2) becomes

$$\sum_{i} \left( E I \varphi_{i}^{(4)} q_{i} + (M + m) \varphi_{i} \ddot{q}_{i} + (\dot{m} + U m') \varphi_{i} \dot{q}_{i} + 2m U \varphi_{i}' \dot{q}_{i} + \left( U^{2} m(L, t) + I(x, t) \right) \varphi_{i}'' q_{i} \right) = 0$$
(4)

The Galerkin method will be used to simplify the equation above. Experimental damping tests have been primarily carried out on first mode vibrations. For this reason we consider a one mode approximation. For analytical simplicity here, we shall also consider a pinned-pinned tube. Putting  $\varphi_1 = \varphi$  and  $q_1 = q$  we obtain

$$\int_{0}^{L} \left( E I q \varphi^{(4)} \varphi + (M + m) \varphi^{2} \ddot{q} + (\dot{m} + U m) \varphi^{2} \dot{q} + 2 m U \varphi^{2} \varphi \dot{q} + \left( U^{2} m(L, t) + I(x, t) \right) \varphi^{2} \varphi \dot{q} \right) dx = 0$$
(5)

Introducing m(x,t) from equation (1) and performing the integrals leads to the following simplified one mode system:

$$\left[M + \frac{(N-1)m_0}{L} + \frac{m_0}{L} \left\{ H(1 - \frac{t}{\beta T}) - P(t) \right\} \right] \ddot{q} + \frac{2\pi U m_0}{L^2} Q(t) \dot{q} + \left(\frac{\pi}{L}\right)^2 \left[ EI\left(\frac{\pi}{L}\right)^2 - U^2 m(L, t) \right] q = 0.$$

$$(6)$$

The periodic functions P(t) and Q(t) capture the periodicity of mass variation within the tube due to passing slugs. To simplify things further, the functions P(t) and Q(t) are represented by their first order Fourier series, leading to

$$\left\{ P(t) - H(1 - \frac{t}{\xi T}) \right\} \simeq \gamma_0 + \gamma_1 \cos \frac{2\pi}{T} t \quad , \quad Q(t) \simeq \alpha_0 + \alpha_1 \sin \frac{2\pi}{T} t \left( \frac{\pi}{2} - \theta \right) \quad , \quad m(L, t) = \frac{m_0}{L} \left( \sigma_0 + \sigma_1 \cos \frac{2\pi}{T} t \right) \tag{7}$$

Equation (6) then takes the form below

$$\left[M + \frac{(N-1)m_0}{L} - \frac{m_0}{L} \left\{ \gamma_0 + \gamma_1 \cos \frac{2\pi}{T} t \right\} \right] \ddot{q} + \frac{2\pi U m_0}{L^2} \left(\alpha_0 + \alpha_1 \sin \frac{2\pi}{T} t\right) \dot{q} + \left(\frac{\pi}{L}\right)^2 \left[EI - \frac{U^2 m_0}{L} \left\{\sigma_0 + \sigma_1 \cos \frac{2\pi}{T} t\right\} \right] q = 0.$$
(8)

Equation (8) shows that the slugs act as parametric excitation to the modal vibrations.

Introducing next the dimensionless parameters below (where  $\varepsilon_1$ ,  $\zeta_0$ ,  $\varepsilon_2$  turn out to be small parameters)

$$\begin{split} \omega &= \frac{2\pi}{T} \approx \frac{2\pi N U}{L}; \qquad \varepsilon_1 = \frac{m_0 \gamma_1}{L} / \left( M + \frac{(N-1)m_0}{L} - \frac{m_0 \gamma_0}{L} \right); \ \zeta_0 = \frac{m_0 \alpha_0}{L} / \left( M + \frac{(N-1)m_0}{L} - \frac{m_0 \gamma_0}{L} \right) \\ \varepsilon_2 &= \frac{m_0 \alpha_1}{L} / \left( M + \frac{(N-1)m_0}{L} - \frac{m_0 \gamma_0}{L} \right); \qquad \varepsilon_3 = \frac{m_0 \sigma_1}{L} / \left( M + \frac{(N-1)m_0}{L} - \frac{m_0 \gamma_0}{L} \right); \\ \omega_0^2 &= \left( \frac{\pi}{L} \right)^2 \left[ EI \left( \frac{\pi}{L} \right)^2 - \frac{m_0 U^2}{L} \sigma_0 \right] / \left( M + \frac{(N-1)m_0}{L} - \frac{m_0 \gamma_0}{L} \right) \end{split}$$

(9)

The following equation, representing a parametrically excited system is obtained:

$$(1 - \varepsilon_1 \cos \omega t) \ddot{q} + \frac{2\pi U}{L} (\xi_0 + \varepsilon_2 \sin \omega t) \dot{q} + \omega_0^2 \left[ 1 + \varepsilon_3 \left( \frac{\pi U}{L \omega_0} \right)^2 \cos \omega t \right] q = 0.$$
(10)

Dividing by  $(1 - \varepsilon_1 \cos \omega t)$  and neglecting second order terms, equation (10) becomes:

$$\ddot{q} + \frac{2\pi U}{L} \left( \xi_0 + \varepsilon_2 \sin \omega t \right) \dot{q} + \omega_0^2 \left[ 1 + \left\{ 1 + \left( \frac{\pi U}{L\omega_0} \right)^2 \right\} \varepsilon_3 \cos \omega t \right] q = 0.$$

Via the following change of variables

$$q(t) = \exp(-\frac{1}{2} \int_{0}^{t} \frac{2\pi U}{L} (\zeta_0 + \varepsilon_2 \sin \omega \tau) d\tau) p(t) = \exp(-\frac{\pi U}{L} \zeta_0 t + \frac{\varepsilon_2}{N} \cos \omega t) p(t)$$

equation (10) takes the simpler form

$$\ddot{p} + \omega_0^2 (1 - \varepsilon \cos \omega t) p = 0$$

(12)

where

$$\varepsilon = \frac{\varepsilon_2}{2N} - \varepsilon_3 \left\{ 1 + \left( \frac{\pi U}{L\omega_0} \right)^2 \right\}$$

The reader will recognize equation (12) as the well known Mathieu's equation for parametric forcing. A perturbation solution of this equation in the non-resonant case leads to the following solution for q(t) after the change of variable (11),

$$q(t) = q(0)e^{-\frac{\pi U}{L}\xi_0 t} \cos \omega_0 t + O(\varepsilon)$$
(13)

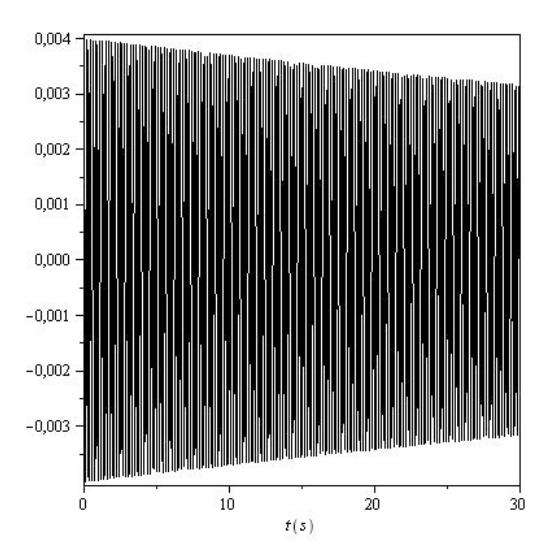
This simplified analytical solution suggests that the force due to the slugs induces an approximate viscous damping like effect on the tube motion. Note that no actual energy dissipation to heat occurs – rather, energy is 'mechanically' transferred to the liquid slugs which then carry it out of the system.

To confirm this result, numerical solution of the non-simplified equations was carried. Figure 4 shows the results of numerical simulations for a flow velocity of 3 m/s and superficial void fraction of 50%. The results clearly show that energy transfer occurs, with the result that the tube response is damped after several cycles. The damping ratio is, however, extremely small at 0.04% - much lower than the measured two-phase damping of 3.43% under the same flow conditions (but for a clamped tube).

Another simulation example is shown in Fig.5. Here the flow velocity is 8 m/s with the superficial void fraction 80%. In this case a higher damping of 0.4% is calculated. Although this damping value is higher, it is still much lower than the experimentally measured damping value of 1.15 %.

The foregoing results suggest that although an energy transfer mechanism between the tube and flow has been found, the amount of energy transferred cannot account for the level of damping observed experimentally. We note also that the trend is also different from that observed in the experiments. These observations have led to a closer inspection of the structure of the slugs during tube vibration. Visual observation coupled with flow visualization showed that during tube free vibrations, the liquid slugs themselves were excited strongly enough to deform periodically at the upper free surface. These

oscillations were all but absent at the bottom of the liquid slug where the concave interface tended to stabilize the free surface.



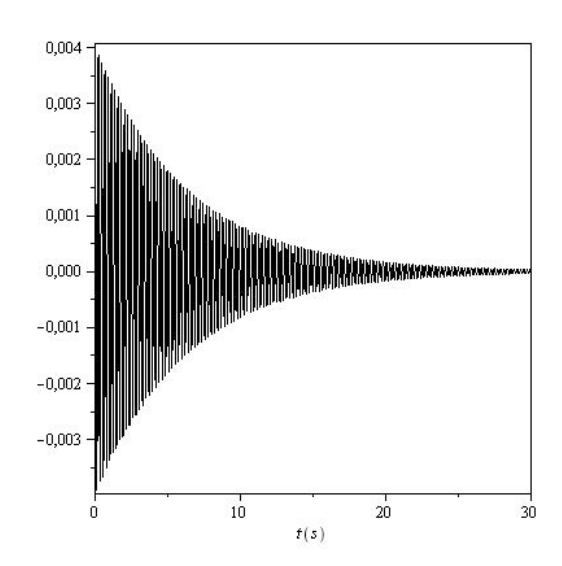


Figure 4 Response for U=3 m/s,  $\beta$ =50%.

Figure 5 Response for U=8 m/s,  $\beta$ =80%.

In the next section then, we incorporate the liquid slug surface dynamics into the theoretical model.

## 2. Sloshing based model

We considered next a more detailed model of fluid motion within the slug itself. In particular, sloshing behavior, associated with the upper free surface of the slugs is of particular interest. As noted earlier, experiments show that the lower free surface (the top of the bubble in Fig.1(a)) has a higher curvature and thus tends to be more stable. For simplicity we therefore assume this surface to be immobile (and flat!). The upper free surface oscillations can be modeled, for a first approximation, as a classical sloshing problem. The problem is more complex now though because the slugs also have a global motion within the tube. The sloshing problem has been addressed by numerous researchers. We follow the approach of [7] to derive a simple first order model for slug sloshing. The resulting oscillating force due to sloshing is then added to the slug-tube interaction forces already considered above.

## 2.1 Equations governing slug sloshing

In this section we briefly outline the basic equations for small amplitude sloshing. An (idealized) individual liquid slug is shown in Fig.6. Flow is upward (against gravity) in the figure and the tube inner diameter is *a*. The fluid motion associated with sloshing is approximated by a potential 'flow' for small tube oscillations.

The equations for the flow potential and boundary conditions are

$$\begin{cases} \frac{\partial^2 \phi}{\partial r^2} + \frac{1}{r} \frac{\partial \phi}{\partial r} + \frac{1}{r^2} \frac{\partial^2 \phi}{\partial \theta^2} + \frac{\partial^2 \phi}{\partial z^2} = 0 \\ \frac{\partial \phi}{\partial r} \Big|_{r=a} = 0, \quad \frac{\partial^2 \phi}{\partial z^2} \Big|_{z=-h} \approx 0 \end{cases}$$

(14)

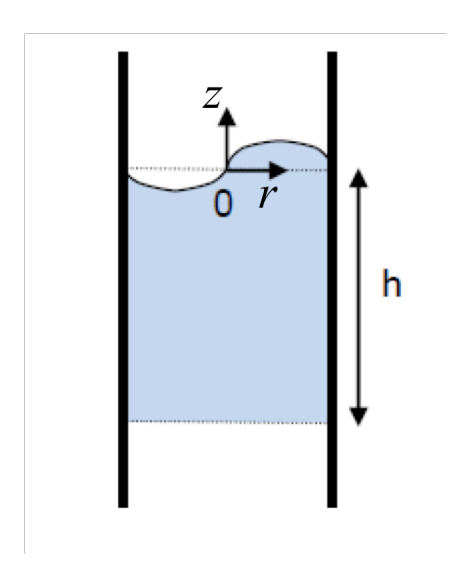


Fig.6 Liquid slug geometry

At the upper free surface (elevation  $z = \eta(r, \theta, t)$ ), the following boundary condition holds

$$\begin{cases}
\frac{\partial \eta}{\partial t} + \frac{\partial \eta}{\partial r} \frac{\partial \phi}{\partial r} + \frac{1}{r} \frac{\partial \eta}{\partial \theta} \frac{\partial \phi}{\partial \theta} = \frac{\partial \phi}{\partial z} \\
\frac{\partial \phi}{\partial t} + \frac{1}{2} \left( \frac{\partial \phi}{\partial r} \right)^2 + \frac{1}{2} \left( \frac{1}{r} \frac{\partial \phi}{\partial \theta} \right)^2 + \frac{1}{2} \left( \frac{\partial \phi}{\partial z} \right)^2 + \ddot{w}_s r \cos \theta + g \eta = 0
\end{cases}$$
(15)

where the subscript 's' in equation (15) indicates that the tube acceleration at the slug location should be considered here. In keeping with low order approximation, the boundary conditions are linearized to give

$$\begin{cases} \frac{\partial \eta}{\partial t} = \frac{\partial \phi}{\partial z} \\ \frac{\partial \phi}{\partial t} + \ddot{w}_s r \cos \theta + g \eta = 0 \end{cases}$$

(16)

Series expansions for the potential function and free surface elevation solutions considering only antisymmetric circumferencial modes are expressed in the form

$$\phi(r,\theta,z,t) = \sum_{n} \sum_{m} A_{nm}(t) \cos(m\theta) J_{n}(\lambda_{n} \frac{r}{a}) \frac{\sinh(\frac{\lambda_{n}}{a}(h+z))}{\sinh(\lambda_{n} \frac{h}{a})}$$
$$\eta(r,\theta,z,t) = \sum_{n} \sum_{m} C_{nm}(t) \cos(m\theta) J_{n}(\lambda_{n} \frac{r}{a})$$

(17)

The series above are injected into equation (14) and simplified boundary conditions (16) and the Galerkin method used to effect the modal projection. Considering only one mode (hence m=n=1), the following equations for the modal generalized coordinate are obtained

$$\dot{C}_{11}(t) = \frac{\omega_1^2}{g} A_{11}(t)$$

$$\dot{A}_{11}(t) = -gC_1(t) - S_1 \ddot{w}(x_s, t)$$
(18)

with:

$$S_1 = \frac{1}{I_1} \int_0^a J_1(\lambda_1 \frac{r}{a}) r^2 dr, \ I_1 = \int_0^a J_1^2(\lambda_1 \frac{r}{a}) r dr, \ \omega_1 = \sqrt{\frac{g\lambda_1}{a} \tanh(\lambda_1 \frac{h}{a})}$$

Note that in equation (18) the tube acceleration is  $\ddot{w}(x_s,t)$  at the slug location  $x_s$ ; the location of each slug will in fact be a function of time,  $x_s = U(t - t_s)$ , where  $t_s$  marks the instance when the slug enters the tube. Equations (18) can be recast in the following form of a standard second order forced oscillator

$$\ddot{C}_{11}(t) + \omega_1^2 C_{11}(t) = -S_1 \frac{\omega_1^2}{g} \ddot{w}(x_s, t)$$

(19)

Solution of equation (19) yields the following expressions potential for the slug oscillation flow potential and surface height

$$\phi(r,\theta,z,t) = A_{11}(t)\cos(\theta)J_1(\lambda_1\frac{r}{a})\frac{\sinh(\frac{\lambda_1}{a}(h+z))}{\sinh(\lambda_1\frac{h}{a})}; \quad A_{11}(t) = \frac{g}{\omega_1^2}\dot{C}_{11}(t)$$

$$\eta(r,\theta,z,t) = C_{11}(t)\cos(\theta)J_1(\lambda_1\frac{r}{a})$$
(20)

# 2.2 Sloshing-induced forces and the fluid-structure problem

With the flow potential (20) known, the force associated with sloshing for each liquid slug may be determined from momentum considerations. The forces consist of two components, one associated with oscillatory pressure variations in the radial (r) direction, the second due to bulk acceleration of the slug. The total force at the axial position is given by the integral

$$F_{s}(x_{s},t) = \int \int \int \rho a \frac{d\vec{V}_{r}}{dt} cos\theta d\Omega + \int \int \int \vec{\Phi} \ddot{w} cos^{2}\theta \vec{e}_{r} d\Omega$$

$$\vec{V}_{r} = \frac{1}{r} \frac{\partial \phi}{\partial \theta}, \int \int \int (.)d\Omega = \int \int_{0}^{2\pi} \int_{0}^{\eta} \int_{0}^{a} (.)d\theta dz dr$$
(21)

To solve equation (19), the tube displacement w(x,t) needs to be known. Since the latter depends also on the slug oscillations, a coupled problem needs to be solved. The fluid-structure problem was outlined earlier in section 1.2. In the tube equation of motion (equation (2)), the first term of the slug force (equation (21)) is added. Note that the second term in equation (21), which is the force due to the bulk acceleration of the slug, is already present in the second term of the fluid-structure interaction equation (2).

The solution of the numerical problem defined by equations (2), (19) and (21) is not trivial since it involves an intro-differential system. The symbolic software MAPLE is used to obtain the numerical solutions. In view of the simplifications already included in the model, no attempt is made to solve the equations simultaneously. Instead, the sloshing and vibrations problems are solved with a delay of one time step which effectively introduces a decoupling (albeit at a frequency much higher than the natural frequency of either system).

# 2.3 Simulations results

The transient response of a clamped-clamped tube is considered for better comparison with experiments. The tube is 1.48m long with an inner diameter a=2.12 cm and wall thickness t=2.8mm. The acrylic tube has a mass of 0.309 kg/m and first model natural frequency of 21 Hz. Fig.7 shows the two-phase damping measured for this tube at a mixture (homogeneous) flow velocity of 1 m/s for a range of void fractions.

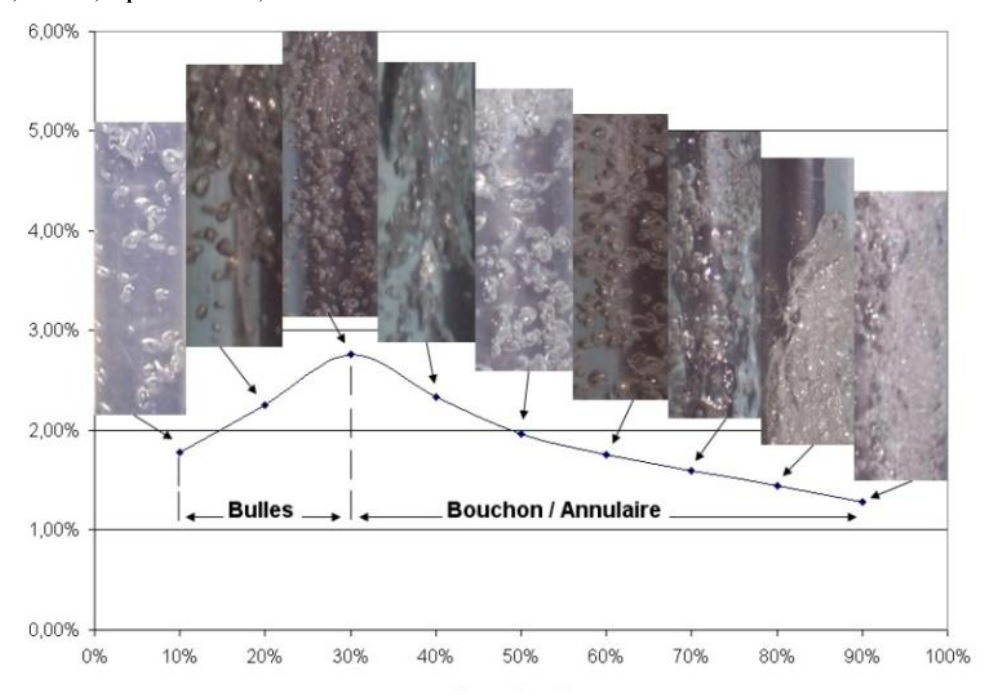


Figure 7 Two phase damping versus void fraction ( $\beta$ %) for a velocity of 1 m/s.

In this case, a maximum damping is found near 30% superficial void fraction. In the slug flow regime the two-phase damping is in the range of 1.5% to just below 3%.

A numerical solution is carried out for this tube and selected conditions in the slug flow regime. Fig.8 shows the numerically computed free vibration response for U=1m/s and void fraction  $\beta=40\%$ . The estimated slug frequency is 4 Hz. The computed two-phase damping due to sloshing is  $\xi=4.47\%$ . The experimentally measured damping for the same flow conditions is  $\xi=2.34\%$ . In Fig.9 a second simulation result is presented for a higher flow velocity of 3 m/s, void fraction  $\beta=50\%$  and an estimated slug frequency of 5 Hz. The calculated damping is  $\xi=2.13\%$  compared to the experimentally measured value of  $\xi=3.43\%$ .

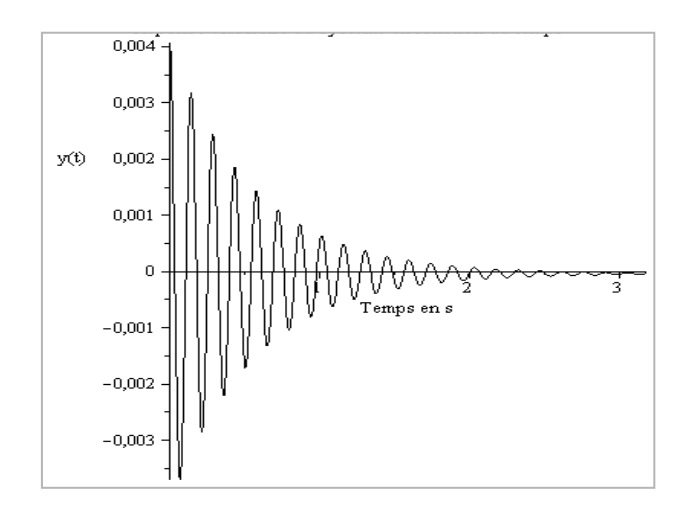


Figure 8 Tube response for U=1 m/s,  $\beta=40\%$ .

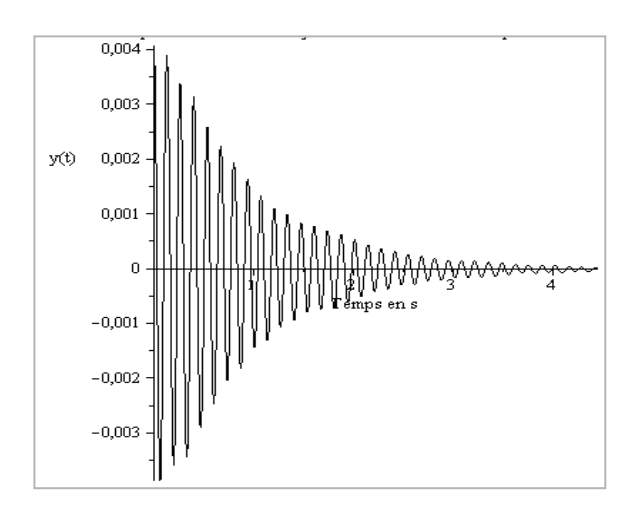


Figure 9 Tube response for U=3m/s,  $\beta=50$ %.

The theoretically estimated damping values fall within the range of experimental measurements. In view of the simplifying assumption, the model can be deemed to be modestly successful in demonstrating that for slug flow, sloshing type free surface motions in the liquid slugs plays a key role in generating 'apparent' two-phase damping. In this case the tube damping effect is a purely inertia related phenomenon with no actual viscous dissipation.

The results demonstrate that the (or a) basic mechanism for slug flow-induced damping is likely closely inertia related and more specifically, sloshing of the slugs themselves. This simple model has a number of limitations. One important input is the slug frequency which is estimated from experimental data. A more elaborate model may take into account the inexact periodicity of slugging. There is also the difficult problem of the exact form of the slugs themselves. The present model idealizes the slugs as depicted in Fig.6. However, as seen in Fig.1 and Fig.7, the slugs have a more complex structure including a significant wake region. The latter means that the slug does not have a constant depth (h) as assumed in the model. Furthermore, the slugs themselves will generally contain gas bubbles which modify the effective slug density. This is another important reason for the difference between the computed and measured damping values.

The authors are aware that there will be limitations to the model since the detailed two-phase flow mechanisms are not considered. An obvious inconsistency of the model, relative to the experiments, is the inverse (decreasing) trend observed in the computed damping compared to the (increasing) trend in the experiments as a function of void fraction. This clearly points to an inconsistency in the model. A possible error is in the estimation of the slugging frequency. More importantly, the flow pattern changes with void fraction – and as figure 7 shows, the definition of a given flow pattern is at best approximate. Despite these short comings, the basic idea, confirmed here, is that the globally observed damping effect is relatively independent of some of the more complex dynamics of the two-phase flow.

#### 3. Conclusion

This work has proposed an analytical model for the estimation of two-phase damping induced by slug flow. Firstly a simple point mass model was developed which showed that propagating slugs — modelled as point masses — can lead to a parametric excitation (damping!) of the containing pipe or tube. The resulting damping was, however, found to be significantly smaller than measured values.

The model was developed further to include a first order approximation of sloshing dynamics within the slugs as a mechanism for the transfer of kinetic energy from the tube to the flow. This sloshing based model was found to give damping values within the range of measured damping values – suggesting that slug sloshing could potentially be an important mechanism for two-phase damping for slug flow. Further work is, however, needed to improve the model for better consistency with experimental measurements.

#### 4. References

- [1] L.N., Carlucci and J.D., Brown, "Experimental studies of damping and hydrodynamic mass of a cylinder in confined two-phase flow", ASME Journal of Vibration, Acoustics, Stress, and Reliability in Design 105, 1983, pp. 83–89.
- [2] M.J., Pettigrew, and C.E., Taylor, "Damping of heat exchanger tubes in two-phase flow: review and design guidelines", ASME Journal of Pressure Vessel Technology 126, 2004, pp. 523–533.

- [3] Hara, F., Kohgo, O., "A theory for a vibrating circular rod damping in two-phase bubbly fluid", Transactions JSME, Vol. 51, 1985, pp.143–148.
- [4] A., Gravelle, A., Ross, M.J., Pettigrew, N.W., Mureithi, "Damping of tubes due to internal two-phase flow", Journal of Fluids and Structures 23, 2007, pp. 447–462.
- [5] J.G. Collier and J.R. Thome, <u>Convective boiling and condensation</u> (3<sup>rd</sup> ed.), Oxford University Press, Oxford, 1994.
- [6] M.P. Paidoussis, Fluid-structure interactions, Vol.1, Elsevier, 1988.
- [7] S. Kaneko, and Y. Mizota, "Dynamical modelling of deepwater-type cylindrical tuned liquid damper with a submerged net", ASME Journal of Pressure Vessel Technology, Vol. 122, 2000, pp. 96-104.